Thermal Decomposition Kinetics of Lead(II) Decanoate

Henry A. Ellis * and Eric K. Okoh
Department of Chemistry, University of Ife, Ile-Ife, Nigeria

The thermal decomposition of lead(II) decanoate has been investigated using thermogravimetry (t.g.) derivative thermogravimetry (d.t.g.), and differential thermal analysis (d.t.a.). The solid products of decomposition are analysed by conventional techniques and the gaseous products by t.g. linked to m.s. and to g.l.c. Kinetic information on thermal decomposition of the melt in the temperature range 520—720 K is obtained from the t.g. curve by the methods of Coates and Redfern, Freeman and Carroll, and Anderson and Freeman. The results are consistent with a diffusion mechanism as the rate-controlling step and activation energy values are presented for overall decomposition and formation of products. Evolved gas analysis shows that whilst the parent ketone, nonadecan-10-one, is the major product of decomposition, lower ketones, alkanes, alkenes, CO_2, and CO are also present in measurable quantities. A mechanism in explanation of the overall decomposition reaction is discussed in the light of these results.

It has long been established that salts of carboxylic acids thermally decompose to yield symmetrical ketones as the major product.[1-3] For example, barium tetradecanoate when heated to temperatures in excess of 473 K produces heptacosan-14-one in good yield.[3] Furthermore, mixed ketones have been prepared in good yield as pyrolysis products from mixed salts of organic acids.[4-5] Though these reactions are well known, their decomposition reaction mechanisms are complicated. For example, Judd and his co-workers[6] found acetone as the major product on pyrolysing calcium acetate but observed acetic acid when calcium was replaced by silver(II). The function of the metal ion is obscure. Indeed, it has been reported that the yield of ketone varies markedly with metal ion when alkali and alkaline earth salts of organic acids are pyrolysed.[7,8] It is not surprising, therefore, that various mechanisms have been advanced in an attempt to explain the degradative route of these compounds.[9-18] However, it seems likely, in view of the non-integral reaction order in the decomposition kinetics,[19,20] and the many products obtained from the pyrolysis of simple organic salts,[17] that a mechanism involving free radicals is most plausible.

In the present work, the thermal decomposition kinetics of molten lead(II) decanoate (PbC_{10}) were studied using thermogravimetry (t.g.) and differential thermogravimetry (d.t.g.). The evolved gases were simultaneously identified by t.g. linked to a mass spectrometer or gas liquid chromatograph. In addition, the system was studied by differential thermal analysis (d.t.a.).

Experimental

The preparation of lead(II) decanoate has been described elsewhere.[21]

Thermogravimetry.—Thermogravimetric experiments were carried out on a Stanton Redcroft TG750 thermobalance on samples in the weight range 3—9 mg in dry nitrogen at a flow rate of 20 cm^3 min^{-1} and a heating rate of 20 K min^{-1}. Changes in sample weight were recorded as a permanent trace on a Servoscribe 2s RE571 *X–Y* recorder. D.t.g. curves were obtained by direct measurement from the output of the thermobalance using a Stanton Redcroft DTG unit.

T.g.–Mass Spectra.–Simultaneous t.g.–mass spectra data were obtained from a Stanton Redcroft TG750 thermobalance interfaced to a V.G. Micromass MM601 mass spectrometer. Runs were performed under helium at 50 cm^3 min^{-1}. The technique has been described elsewhere.[22]

T.g.–Gas Liquid Chromatography.—Data were obtained under flowing oxygen-free nitrogen from a TG750 thermobalance linked to a Pye–Unicam 104 gas chromatograph *via* a heated glass-lined capillary (i.d. 0.4 mm). The gas chromatograph column was a 1.83 m × 6.35 mm i.d. stainless steel tube packed with 100—120 mesh universal support coated with 10% Apiezon. Column, injector, and detector temperatures were 493, 513, and 543 K, respectively. Chromatograms were obtained by the injection of evolved gas samples at the maximum rate of decomposition as determined by d.t.g.

D.t.a.—D.t.a. curves were obtained from a Stanton Redcroft differential thermal analyser, type 673, on samples in the weight range 5—10 mg in a dynamic atmosphere of dry nitrogen.

Results and Discussion

The t.g., d.t.g., and d.t.a. curves for the thermal decomposition of PbC_{10} are shown in Figure 1. Both t.g. and d.t.g. curves show decomposition to be a two-stage process. However, the d.t.a. curve shows an extra sharp endotherm, prior to decomposition, at 385 K. This endotherm is not associated with a weight change and has been assigned by Adeosun and Sime [23] as the melting endotherm for this compound. The endotherms at 594 and 664 K are as expected associated with weight changes in the compound.

The first stage of decomposition began at *ca.* 465 K (sometimes described as the threshold decomposition temperature) and was over after *ca.* 28% weight loss at *ca.* 638 K. The second stage was complete after 59% weight loss, indicative of the oxide as the final decomposition product (PbO requires 40.64% weight remaining; obtained 41%). The partially decomposed solid obtained at *ca.* 573 K from a separate pyrolysis in a long cylindrical Pyrex tube under flowing nitrogen was separated into its inorganic and organic components by extraction in ether and methanol. Lead carbonate was identified as a component of the inorganic extract by the positive identification of carbon dioxide as the gas evolved when the inorganic residue was partially dissolved in dilute acetic acid. The dark brown organic extract, after work-up in ether and methanol, yielded three separate crystalline compounds. I.r. analyses of these suggested that they were all carbonyl compounds because of the presence, in each, of a strong 1 745 cm^{-1} carbonyl absorption and a medium—strong absorption in the region 1 410—1 440 cm^{-1}, possibly due to the presence of $-CH_2-CO-$. The compounds were tentatively assigned as ketones because of the absence of formyl absorptions in the

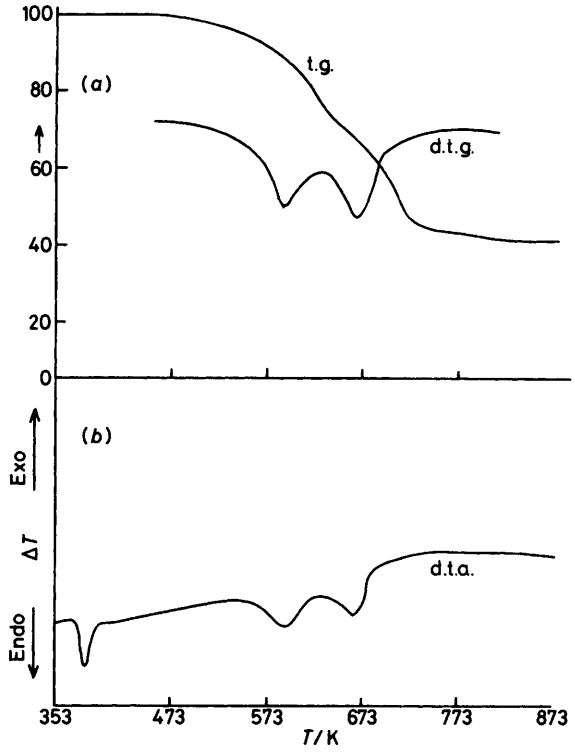

Figure 1. (*a*) T.g., d.t.g., and (*b*) d.t.a. curves for PbC_{10}

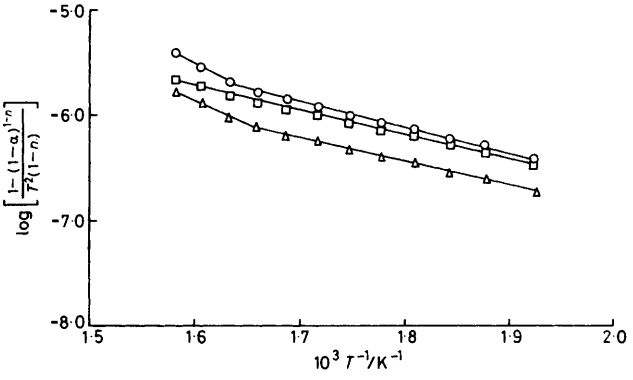

Figure 2. Coates–Redfern kinetic plots for the decomposition of PbC_{10}: ○, $n = \frac{2}{3}$; □, $n = 0$; △, $n = \frac{1}{2}$

region 2 700—2 900 cm^{-1}. Further support for this assignment was provided by the n.m.r. spectra where, in each case, typical methyl group protons attached to an adjacent carbon atom were obtained at δ 0.82 and methylene group protons attached to a carbonyl group at δ 2.35. Whilst the major organic fraction (*ca.* 70%) was positively identified as nonadecan-10-one by a sharp m.p. at 55—56 °C (lit.,[24] 55—57 °C) and by elemental analysis (Found: C, 80.05; H, 13.95. Calc. for $C_{19}H_{33}O$: C, 80.7; H, 13.45%), the other compounds melted over a wide temperature range and are considered to be mixtures.

The α–time plots, where α is the fraction of substance decomposed after time *t*, are typically sigmoidal for both stages of decomposition. This suggests that the rates of reaction are controlled either by a diffusion mechanism, a contracting reaction interface, or by the remaining amount of reactant.

Rising-temperature kinetic data were obtained from the t.g. curve by the methods of Coates and Redfern,[25] Freeman and Carroll,[26] and Anderson and Freeman.[27] The Coates and Redfern method assumes a rate law of type (1) where $k = Ae^{-E/RT}$; *n* is the order of reaction, *E* the activation energy,

$$d\alpha/dT = k(1 - \alpha)^n \quad (1)$$

A the frequency factor, *R* the gas constant, and *T* the absolute temperature. The activation energy for decomposition is obtained from a plot of $\log \{[1 - (1 - \alpha)^{1-n}]/T^2(1 - n)\}$ *versus* $1/T$ at the value of *n* where such a plot becomes linear. The plots for the first stage of decomposition are shown in Figure 2 and the kinetic data presented in Table 1. The plots show that the relationship in Figure 2 is satisfied when the order of the reaction is zero. Though the first stage of reaction could be easily analysed, the second stage of decomposition presented a more complex picture. A precise value of *n* could not be found to give a linear plot and therefore no useful kinetic data could be obtained for this stage of decomposition.

Table 1. Kinetic data for PbC_{10} decomposition under nitrogen

Kinetic method	α	*n*	*E*/kJ mol^{-1}	*T*/K
Coates–Redfern	0.1—0.9	0	41.74 ± 1.0	520—633
				633—703
Freeman–Carroll		0.07 ± 0.2	42.05 ± 2.3	483—633
Anderson–Freeman		0	4.74 ± 0.22	483—573
			18.87 ± 2.0	583—613
			28.48 ± 3.0	653—713

The Freeman–Carroll–Anderson methods assume a common rate law of type (2) where *X* is the amount of reactant.

$$-dX/dt = kX^n \quad (2)$$

From this simple expression, the well known Freeman–Carroll expression is derived. The kinetic results so obtained are also presented in Table 1. The activation energy values determined by the two methods so far described are in very good agreement. Furthermore, both methods of analysis describe zero-order kinetics. These results are in very good agreement with those obtained by Rasheed and Bhobe [28] (*E ca.* 41 kJ mol^{-1}; *n* 0) for the thermal decomposition of zinc octadecanoate, suggestive of similarities in the chemistry of these divalent metal carboxylates.

Whilst the kinetic methods discussed so far describe, fairly well, the overall kinetics of decomposition, the Anderson–Freeman method claims to be more sensitive to changes in activation energy and reaction order during decomposition. This method is based on expression (3) where dw/dt is the

$$\Delta\log(dw/dt) = n\Delta\log Wr - (E/2.3R)\Delta(1/T) \quad (3)$$

rate of reaction, determined from tangents to the weight loss curve; $Wr = \Delta W_c - \Delta W$, where ΔW_c is the total weight loss associated with a given reaction and ΔW, the weight loss at the point where dw/dt is taken. From the plot of $\Delta\log(dw/dt)$ *versus* $\Delta\log Wr$ at constant $\Delta(1/T)$, the order of reaction is determined from the slope and the activation energy from the intercept at $\Delta\log Wr = 0$. Both dw/dt and *Wr* were first determined from the plot of dw/dt and *Wr versus* the reciprocal of the absolute temperature. The initial points representing *ca.* 28% of reaction up to 633 K did not fall on a straight line. The Arrhenius plot, depicted in Figure 3, indicates zero-order kinetics up to this stage of decomposition. Additionally, the plot shows that there are two activation processes occurring over this range. The first process occurs over the first 8—9% of decomposition and the other over the next 9—28% with activation energies of 4.74 and 18.87 kJ mol^{-1}, respectively

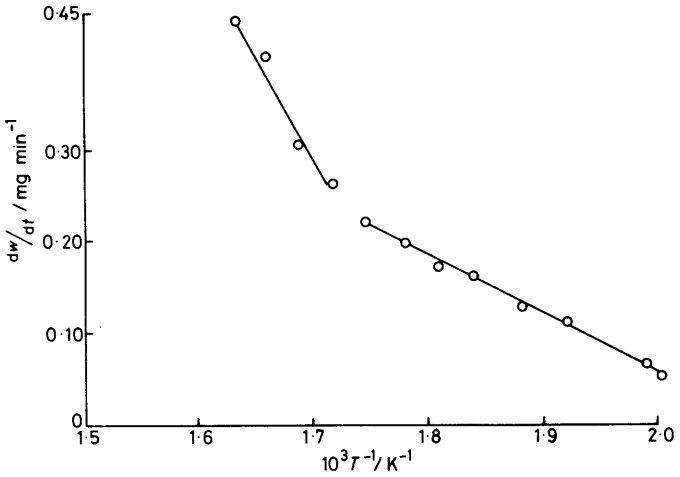

Figure 3. Anderson–Freeman Arrhenius plots for PbC_{10} decomposition

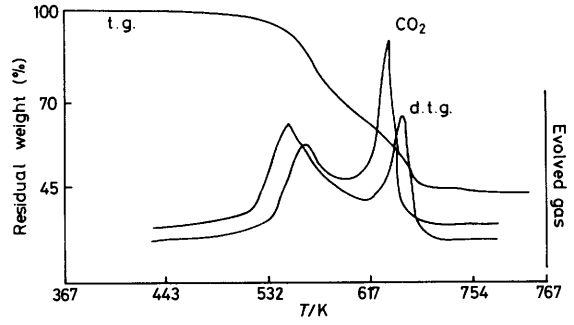

Figure 4. Simultaneous t.g., d.t.g., and evolved gas curves for PbC_{10}

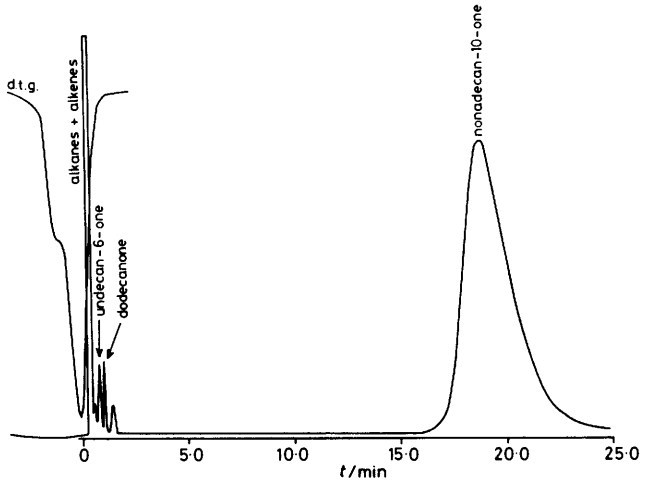

Figure 5. Chromatogram of decomposition products obtained at *ca.* 663 K

(Table 1). Zero-order kinetics is also indicated for the second stage of decomposition. The overall activation energy of 52.09 ± 5 kJ mol^{-1} is somewhat, though not unreasonably, high and is probably a reflection of the large errors involved in the extrapolation procedure. However, it is pleasing to note that all the kinetic methods of analysis indicate zero-order kinetics for the first stage of decomposition.

Whilst zero-order kinetics are in good agreement with previous work on the higher lead carboxylates,[18] this order of reaction is somewhat different from the corresponding sodium carboxylates. Stephenson and Pearson [20] obtained orders of reaction of two-thirds for the even chain-length Na C_6—C_{16} carboxylates inclusively. This is not surprising in view of the demonstrable differences in their melt structures and physical properties. For example, though sodium [29] and lead [23] carboxylates, on heating, form intermediate phases between the solid and melt, they differ in the larger number of phase transitions for sodium and the occurrence of an isotropic liquid phase in the case of lead and a reversed hexagonal phase in the case of sodium as the high-temperature phase. Furthermore, their final decomposition products are different; the oxide is formed in the lead case and the carbonate in the sodium case. In addition, the sodium threshold decomposition temperatures are generally *ca.* 200 K higher than lead. These differences are due in part to difference in metal ion size and in co-ordination around the different metal ions.

The kinetic results, here obtained, indicate that decomposition up to at least 28% of reaction is controlled by diffusion of products from the surface of PbC_{10}, *i.e.* in the initial stages of reaction, the surface of PbC_{10} is completely covered by product molecules. The activation energy value of 4.74 kJ mol^{-1} for the first 8—9% of decomposition is most probably representative of the desorption of a gaseous product from the surface of the molten soap. A weight loss of this magnitude suggests that carbon dioxide is most probably the major product of reaction up to 573 K.

Table 2. G.l.c. analysis of decomposition products at *ca.* 663 K

Compounds	Relative yield (%)
Alkanes + alkenes	*ca.* 15
Decanone (tentative)	0.5
Undecan-6-one	1.2
Dodecanone	1.2
Tridecanone (tentative)	0.8
Nonadecan-10-one	100

The presence of carbon dioxide as a product of reaction is confirmed by simultaneous t.g.–m.s. in the peak select mode at a mass peak of 44 (Figure 4). The results show that carbon dioxide is evolved in two stages up to 645 K, corresponding to the two stages of decomposition. The decarboxylation reaction can be attributed to the decarboxylation of lead carbonate

($PbCO_3$). Evidence for $PbCO_3$ decarboxylation of this type is provided by the work of Warne and Bayliss [30] on the thermal decomposition of pure $PbCO_3$. These workers were able to show that decarboxylation occurred in three stages over the temperature range 613—713 K, through a series of PbO and $PbCO_3$ intermediates.

The d.t.g.–g.l.c. results are shown in Figure 5 and the relative yields of compounds as a percentage of the major product presented in Table 2. The results indicate that the most abundant decomposition products are nonadecan-10-one, alkanes, and alkenes; minor products are decanone (tentatively assigned), undecan-6-one, dodecanone, and tridecanone (tentatively assigned). Furthermore, the evolved gas analysis data of both the first and second stage of decomposition, obtained by injecting a single evolved gas sample onto the g.l.c. column at the first and second maxima of the rate of decomposition, as suggested by d.t.g. experiments, showed that the same products were obtained for both stages of decomposition. From the g.l.c. results, it is tempting to suggest that the plateau on the t.g. curve (Figure 1) at *ca.* 638 K might be as a result of some physical phenomenon such as the coverage of the surface of the melt by $PbCO_3$ or some such complex. Such an idea is not unreasonable because of the heterogeneous nature of the decomposition reaction where the Scheme is envisaged. Such a Scheme has, indeed,

$$PbC_{10(s)} \xrightarrow{heat} PbC_{10(l)} \xrightarrow{heat} \text{solid} + \text{gas}$$

Scheme

been advanced to explain two-stage decomposition in other carboxylates.[31] This phenomenon appears, from the limited data available, to be confined to smaller carboxylates like PbC_{10}, PbC_{12}, and PbC_{14} and not PbC_{18}, where decomposition occurs in a single step. Furthermore, support for this view is provided by the Coates–Redfern plot for the second stage of decomposition where a value of n could not be found, probably because of the insensitive nature of this method. Nevertheless, the Anderson–Freeman analysis indicated that both stages of decomposition were of the same zero order and this, taken in conjunction with the evolved gas data, support a single degradative process.

The peak labelled alkanes and alkenes in Figure 5 is identified as a mixture of normal alkanes and monoalkenes from simultaneous t.g.–m.s. The identification is based on characteristic ions at *m/e* 41, 43, 55, 57, *etc.* Since the thermobalance was initially purged with helium until the mass spectrometer indicated a constant low level of oxygen, peak heights at *m/e* 28 [identified as carbon monoxide (CO) and distinguished from nitrogen by the relative abundance of the CO $M + 2$ peak], 41, 43, 55, and 57 are plotted as a function of decomposition temperature (Figure 6). The lower alkanes and alkenes are observed to increase smoothly with temperature up to *ca.* 613 K when they decrease above this temperature. Though CO has been shown [9,20] as a product of carboxylate decomposition, and the results here confirm this, an interesting feature of these results, contrary to expectation, is the evolution of CO with CO_2. These results suggest that direct metal oxide formation *via* an ionic mechanism, originally postulated by us, is an oversimplification.

In view of the many products formed in this decomposition, and from detailed study of like systems such as calcium butanoate [31] and calcium decanoate [17] where a radical mechanism is postulated for product formation, it is not unreasonable to suggest that a radical mechanism is also operative in this system. Strong claims for other mechanisms have been made by several workers [9,11,15,16] but because these were based on an incomplete analysis of the decomposition products, they should be treated with some caution.

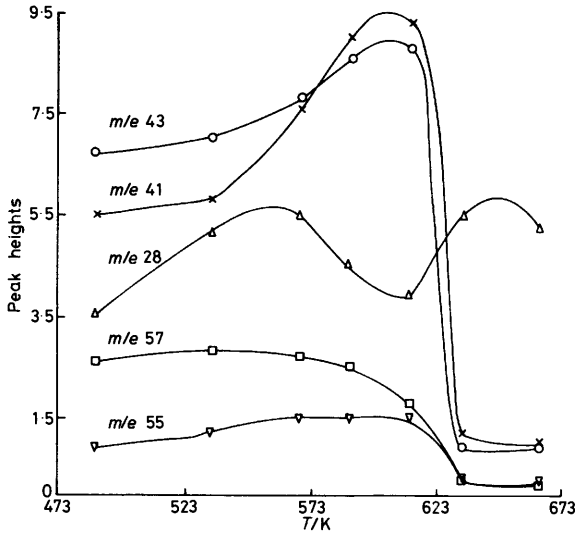

Figure 6. Plots of peak heights obtained from m.s. against temperature

Taking the results of all the product analyses together, it seems reasonable to postulate that the first step (4) in the reaction involves the formation of both alkyl and acyl radicals from PbC_{10}. Lead carbonate can then decarboxylate to PbO

$$(C_9H_{19}COO)_2Pb \longrightarrow {}^{\cdot}C_9H_{19} + C_9H_{19}\dot{C}{=}O + PbCO_3 \quad (4)$$

and CO_2. The major product, nonadecan-10-one, is then formed by the combination of nonyl and decanoyl radicals [reaction (5)]. Furthermore, nonyl radicals could give rise to

$$C_9H_{19}\dot{C}{=}O - {}^{\cdot}C_9H_{19} \longrightarrow C_9H_{19}COC_9H_{19} \quad (5)$$

$$2{}^{\cdot}C_9H_{19} \longrightarrow C_9H_{20} + C_9H_{18} \quad (6)$$

nonane and nonene by disproportionation [reaction (6)]. Smaller alkyl radicals could result from a nonyl radical by a concerted process and β-scission. These radicals may then disproportionate to give alkanes and alkenes or combine to produce alkanes. The presence of smaller ketones such as decanone and tridecanone suggests that decanoyl radical, apart from decomposing readily to CO [reaction (7)], might also

$$C_9H_{19}C{=}O \longrightarrow {}^{\cdot}C_9H_{19} + CO \quad (7)$$

break down to give smaller acyl radicals which can then combine with alkyl radicals. Conversely, these ketones may form from secondary reactions of nonadecan-10-one. Since these compounds are just above 1% of the major product these reactions must occur to a limited extent.

Acknowledgements

We thank Dr. P. A. Barnes and Mr. S. B. Warrington, Leeds Polytechnic, for assistance with the t.g.–m.s. system and Mr. D. K. Stephenson, Huddersfield Polytechnic, for assistance with the g.l.c. work. Useful discussions with colleagues are gratefully acknowledged.

References

1 J. Kenner and F. Morton, *Ber.*, 1939, **72**, 452.
2 J. Kenner and R. L. Wain, *Ber.*, 1939, **72**, 456.
3 S. H. Piper, A. C. Chibnall, S. J. Hopkins, A. Pollard, J. A. B. Smith, and E. F. Williams, *Biochem. J.*, 1931, **25**, 2072.

4 E. B. Ludlam, *J. Chem. Soc.*, 1902, **81**, 1185.
5 C. Granito and H. P. Schultz, *J. Org. Chem.*, 1963, **28**, 879.
6 M. D. Judd, B. A. Plunkett, and M. I. Pope, *J. Therm. Anal.*, 1974, **6**, 555.
7 C. A. Rojan and Jos. Schulten, *Ber.*, 1926, **59**, 499.
8 R. Kronig, *Angew. Chem.*, 1924, **37**, 667.
9 A. L. Miller, N. C. Cook, and F. C. Whitmore, *J. Am. Chem. Soc.*, 1950, **72**, 2732.
10 J. Bell and R. I. Reed, *J. Chem. Soc.*, 1952, 1383.
11 C. C. Lee and J. W. T. Spinks, *J. Org. Chem.*, 1953, **18**, 1079.
12 C. C. Lee and J. W. T. Spinks, *Can. J. Chem.*, 1953, **31**, 103.
13 R. I. Reed, *J. Chem. Soc.*, 1955, 4423.
14 R. I. Reed and M. B. Thomley, *J. Chem. Soc.*, 1957, 3714.
15 L. Otvos and L. Noszko, *Tetrahedron Lett.*, 1960, 19.
16 A. M. Rubinshtein and V. I. Yakerson, *Kinet. Katal.*, 1961, **2**, 118.
17 R. A. Hites and K. Biemann, *J. Am. Chem. Soc.*, 1972, **94**, 5772.
18 H. A. Ellis, *Thermochim. Acta*, 1981, **47**, 261.
19 R. I. Reed, *J. Chem. Phys.*, 1953, **21**, 377.
20 J. T. Pearson and D. K. Stephenson, ' Proceedings of the Second European Symposium on Thermal Analysis,' ed. D. Dollimore, Heyden, London, 1981, p. 298.
21 N. E. Ekwunife, M. U. Nwachukwu, F. P. Rinehart, and S. J. Sime, *J. Chem. Soc., Faraday Trans. 1*, 1974, 1432.
22 P. A. Barnes, G. Stevenson, and S. B. Warrington, ref. 20, p. 47.
23 S. O. Adeosun and S. J. Sime, *Thermochim. Acta*, 1976, **17**, 351.
24 ' The Aldrich Library of Infrared Spectra,' ed. C. J. Pouchert, Aldrich Chemical Co., 1975, 2nd edn., p. 219.
25 A. W. Coates and J. P. Redfern, *Nature (London)*, 1964, **201**, 68.
26 E. S. Freeman and B. Carroll, *J. Phys. Chem.*, 1958, **62**, 394.
27 D. A. Anderson and E. S. Freeman, *J. Polym. Sci.*, 1961, **54**, 253.
28 A. Rasheed and R. A. Bhobe, *J. Indian Chem. Soc.*, 1976, *LIII*, 442.
29 A. E. Skoulios and V. Luzzati, *Acta Crystallogr.*, 1961, **14**, 278.
30 See for example ' Differential Thermal Analysis,' ed. R. C. MacKenzie, Academic Press, London, 1970, vol. I, p. 332.
31 G. Stephenson, Ph.D. Thesis, Leeds Polytechnic, 1981.

Received 28*th April* 1982; *Paper* 2/006